An AA-Sized Vibration-Based Microgenerator for Wireless Sensors

This vibration-to-electrical transducer has an AA-size form factor and generates a DC voltage that can power off-the-shelf integrated circuits.

Steve C.L. Yuen, Johnny M.H. Lee, Wen J. Li, and Philip H.W. Leong
Chinese University of Hong Kong

Electrical chemical batteries power most modern, portable electronic devices. Such batteries require replacement or charging once consumed. So, nonexhaustive power sources would be more convenient. One readily available option is vibration energy. Even though the power from miniature vibration-based generators is very small, improvements in integrated circuit (IC) technology have made miniaturized vibration-powered systems feasible. Vibration-powered wireless sensors obtain power from machine vibrations, human movement, or other forms of motion. These sensors could soon play an important role, particularly in monitoring applications in which battery replacement is inconvenient. Eventually, if such systems' efficiency continually improves, vibration might be able to provide power for mainstream pervasive computing devices.

Here, we demonstrate the feasibility of incorporating micro power transducers (MPTs) with a voltage multiplier and rectifier to make a micro power generator (MPG) that is the same size and shape as an AA battery. The AA-sized module includes a voltage multiplier and a large capacitor to produce the DC output. To find the most energy-efficient voltage multiplier to use with this MPG, we use PSpice simulations to analyze the performance of a doubler, a tripler, and a quadrupler circuit in terms of input power, energy efficiency, and charge time. A startup circuit and a regulator, which are external to the MPG module, apply regulated power to an application circuit after the MPG's voltage output exceeds a preset threshold.

We've used the MPG with the startup circuit and the regulator in a vibration-powered wireless thermometer system, which can transmit temperature measurements every 20 seconds when continuous vibrations with an input acceleration of 4.63 m/s^2 and a frequency of 70.5 Hz are present. We chose the combination of storage capacitor size and comparator threshold voltage so that the regulator applies power to the application circuit when sufficient energy is available for reliable operation. When the vibration is insufficient to drive the application circuit, the startup circuit gracefully shuts down this application circuit; it resumes when the storage capacitor has sufficient energy for operation. The application has a total power consumption of 27.6 μW, which the MPG completely delivers. To the best of our knowledge, our MPG is the smallest vibration-to-electrical transducer that can power off-the-shelf ICs. It weighs 10.5 g, about half the weight of a typical alkaline cell. (The "Comparison with Other Induction-Based Microgenerators" sidebar compares this MPG with other induction-based implementations.)

Micro power transducers

The MPG consists of two MPTs and a voltage multiplier circuit. You can connect the MPTs in series or in parallel, depending on whether you

Published by the IEEE CS and IEEE ComSoc ■ 1536-1268/07/$20.00 © 2007 IEEE

Comparison with Other Induction-Based Microgenerators

Compared to the previously reported induction-based implementations of C.B. Williams and his colleagues[1] or Rajeevah Amirtharajah and Anantha Chandrakasan,[2] our system achieves 3.5 to 20 times better power density. Also, it's possible to manufacture our mechanical resonating springs using an electroplating technique compatible with microelectromechanical systems. This feature has an advantage over commercial systems such as Perpetuum and Ferro Solutions for volume manufacturing and enables precise tuning of mechanical resonating frequencies. When combined with a voltage multiplier and AC-to-DC conversion circuitry, the mechanical resonator fits in a standard AA-sized form factor package for vibration-to-electrical power conversion. A standard 2500 mA-hr, 1.5 V AA battery could operate circuitry drawing 27.6 μW for approximately 15 years, so this type of technology is best suited for low-power applications where battery replacement is difficult.

Shad Roundy developed piezoelectric generators,[3] which provide better power density and higher voltages. Roundy used his generator to drive the University of California, Berkeley's MICA mote node (a mote is a low-power computing node), but turning on the MICA node's power switch for first-time activation requires human intervention. In our micro power generator, the startup circuit handles this electronically. Furthermore, a continuous-vibration source must be available to operate Roundy's generator, whereas ours degrades gracefully when the voltage is insufficient. Although Nathan Schenck and Joseph Paradiso have developed a scheme that includes a startup circuit for a piezoelectric-based generator,[4] our startup circuit uses hysteresis and the designer can precisely set the turn-on and turn-off points via resistors.

REFERENCES

1. C.B. Williams et al., "Development of an Electromagnetic Microgenerator," *IEE Proc. Circuits, Devices and Systems*, vol. 148, no. 6, 2001, pp. 337–342.
2. R. Amirtharajah and A.P. Chandrakasan, "Self-Powered Signal Processing Using Vibration-Based Power Generation," IEEE J. Solid-State Circuits, vol. 33, no. 5, 1998, pp. 687–695.
3. S.J. Roundy, Energy Scavenging for Wireless Sensor Nodes with a Focus on Vibration to Electrical Conversion, doctoral dissertation, Dept. of Mechanical Eng., Univ. of California, Berkeley, 2003; http://engnet.anu.edu.au/DEpeople/Shad.Roundy/paper/ShadThesis.pdf.
4. N.S. Schenck and J.A. Paradiso, "Energy Scavenging with Shoe-Mounted Piezoelectrics," IEEE Micro, vol. 21, no. 3, 2001, pp. 30–42.

want a higher output current or voltage. The MPT is the key component to convert ambient mechanical energy from vibration energy to electrical energy.[1] It contains an inner housing, a microelectromechanical systems (MEMS) spring with spring constant k, an N45-grading rare-earth permanent magnet with mass m and magnetic field intensity B, and a copper coil of length l. The inner housing secures the spring with an attached magnet. Figure 1a shows the key components. Figure 1b shows the outer and inner housing, the magnet, and the resonating spring; the principle is similar to that of a shake-driven flashlight.

The MPT generates AC power when the system vibrates. If the generator housing vibrates with amplitude Y_t, the magnet vibrates with amplitude Z_t. The relative movement between these two vibrating parts causes magnetic flux lines to cut through the coil, inducing voltage in the coil loop according to Faraday's law of electromagnetic induction. The system's average power output P is

$$P = \frac{m\xi_e Y_0^2 \left(\frac{\omega}{\omega_n}\right)^3 \omega^3}{\left[1-\left(\frac{\omega}{\omega_n}\right)^2\right]^2 + \left(2\xi\frac{\omega}{\omega_n}\right)^2} \quad (1)$$

where $\xi_e = (Bl)^2/(2Rm\omega_n)$ is the electrical damping factor, R is the load resistance, Y_0 is the input vibration amplitude, ω is the input vibration angular frequency, and ω_n is the spring-mass system's natural resonance frequency. $\xi = \xi_m + \xi_e$ is the system damping factor, $\xi_m = d/(2m\omega_n)$ is the mechanical damping factor, and d is the mechanical damping ratio.[2] At resonance, maximizing the average power and voltage output gives

$$P = \frac{m\xi_e Y_0^2 \omega_n^3}{4\xi^2} \quad (2)$$

$$V = \frac{BlY_0\omega_n}{2\xi} \quad (3)$$

For an MPT using an electroplated copper spring, some approximate typical parameters include spring constant $k = 40$ N/m, $N45$ magnet with mass 192 mg, first-mode resonance frequency $f_1 = 72$ Hz = 456 radians, damping ratio $d = 0.01$, system damping ratio $\xi = 0.723$, magnetic field intensity $B = 0.36$ tesla (3,600 gauss), coil length $l = 30$ m ($\approx$ 1,700 turns), and input vibration amplitude $Y_0 = 200$ μm.

The MPT's key design issue is how to control the resonance frequency via the spring shape and material. After studying various materials, we found that copper was best because it has a relatively

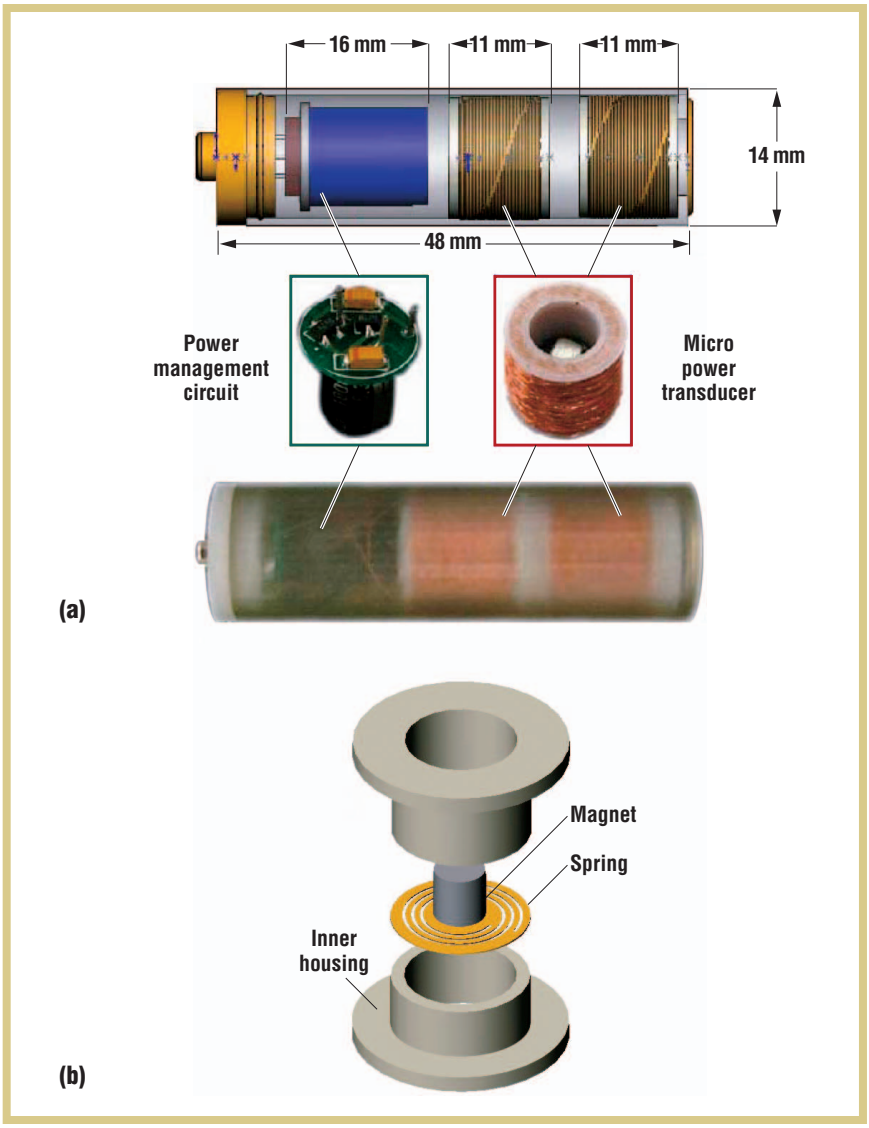

Figure 1. Micro power generator: (a) the power management circuit (which consists of a voltage multiplier and a storage capacitor) and the MPT (with the magnet in the center), and an assembled AA-sized MPG containing the power management circuit and two MPTs; and (b) the micro power transducer's inner structure, showing the coil wound around the inner housing.

low Young's modulus and a high yield stress compared to silicon. Brass, titanium, and 55-Ni-45-Ti are alternatives for different applications; for example, 55-Ni-45-Ti would be suitable for situations requiring a lower resonance frequency. We selected a resonance frequency of 70 Hz on the basis of the available materials, their mechanical strength, the packaging-size constraints, and our desire to optimize the MPT's power density through equation 3. Possible vibration sources with a frequency of approximately 70 Hz include the base of a 5-horsepower, three-axis machine tool with a 36-inch bed (10 m/s^2 maximum acceleration), high-volume air conditioning (HVAC) vents in an office building (1.5 m/s^2), and a notebook computer reading a CD (0.6 m/s^2).[3] An example of an application consistent with these design parameters is monitoring a machine tool's operating temperature.

We used a *high-aspect-ratio MEMS electroplating* technique to manufacture a spiral spring. With this process, you can make springs as thick as 150 µm. First, we put a gold layer on the substrate; this layer acts as a *conducting seed layer* for the copper electroplating station. We then used a lithographic technique to secure an SU-8 negative photoresist mold on the gold layer. After electroplating the copper, we released the spring from the substrate. This lithographic electroplating technique can produce springs that are thinner and have smoother edges than those produced through laser cutting, resulting in a lower, more precise resonance frequency. A lithographic process is also more suitable for mass production because you can make many springs simultaneously in a single batch. Figure 2 shows scanning electron microscope images of an electroplated spring.

Voltage multiplier

Each MPT's AC output voltage, V_{rms} = 450 mV, can't directly drive a conventional digital circuit. Therefore, we introduced a voltage multiplier to step up and rectify the two MPTs' AC outputs (connected in series) to produce a DC output.[4] Figure 3 shows circuit diagrams for the three multipliers we analyzed.

We built a prototype circuit using 10 µF, 10 V capacitors (KEMET type T491) and Toshiba 1SS374 silicon epitaxial Schottky barrier diodes. We chose the 1SS374 diode because it has a low forward voltage (0.23 V), and we chose the capacitor for its size and low leakage. A 1,000 µF Panasonic FC series aluminum electrolytic capacitor (diameter = 10 mm, height = 12 mm) stores the MPG-generated electrical energy and smooths out the voltage multiplier's output.

Startup circuit

The startup circuit applies power to an application circuit only after the

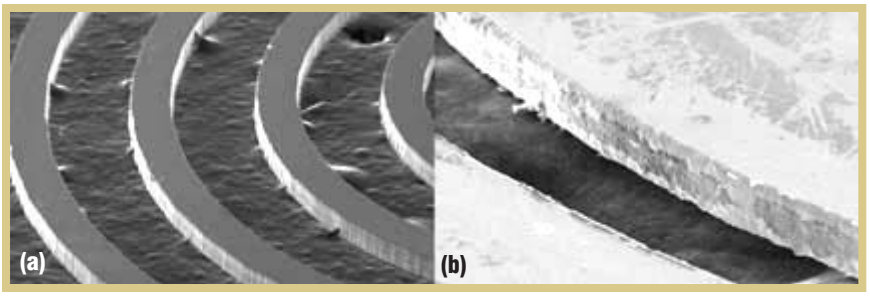

Figure 2. Images of an electroplated spring, from a scanning electron microscope: (a) low and (b) high magnification.

MPG's voltage output exceeds a preset high threshold voltage, $V_{th}(H)$. Without the startup circuit, the application circuit would begin to operate and consume a large current well before the MPG's output reached the minimum voltage required for correct operation. The voltage multiplier's output voltage then wouldn't be able to continue rising.

The startup circuit in figure 4 is a comparator with hysteresis. The comparator's negative reference voltage, along with the three resistors connected to the comparator's positive input, sets its hysteresis—that is, the values of high threshold voltage $V_{th}(H)$ and low threshold voltage $V_{th}(L)$.[5] The startup circuit's output switches the NMOS transistor on when the supply voltage exceeds $V_{th}(H)$ and switches that transistor off when the supply voltage drops below $V_{th}(L)$. When that transistor turns on, the startup circuit provides a return path between the application circuit's system ground and the power ground.

Figure 5 shows the startup transient response of the startup circuit and the system supply. The startup circuit's input capacitor must be large enough to provide sufficient energy for at least one activation of the application circuit. For example, a wireless RF thermometer (described later) consumed 212.62 µJ per activation. So, a 1,000 µF capacitor is sufficient, because the amount of energy available in a charged 1,000 µF capacitor with $V_{th}(L) = 1.4$ V and $V_{th}(H) = 1.9$ V is

$$\begin{aligned} E &= \int_0^\infty iv\,dt \\ &= \int_0^\infty \left(C\frac{dv}{dt}\right)v\,dt \\ &= C\int_{V_{th}(L)}^{V_{th}(H)} v\,dv \\ &= \left\{\frac{C}{2}\left[V_{th}(H)\right]^2 - \left[V_{th}(L)\right]^2\right\} \\ &= 825\,\mu J \end{aligned} \quad (4)$$

MPG model

We tested the MPG and the startup circuit using a vibration drum and a signal generator. The vibration frequency was 70.5 Hz, and we measured the input acceleration as approximately 4.63 m/s^2 using an accelerometer attached to the vibration drum. The amplitude, according to a laser vibrometer, was 250 µm. Using a stroboscope and an oscilloscope, we observed two transducers. The system generated the most energy when the magnets in the MPTs experienced both translational and rotational vibration. This vibration mode provides the highest rate of change in magnetic flux.

Using varying resistive loads, we measured the voltage-current characteristics of two coils in series. The output power was 20 to 120 µW for 1 kΩ to 30 kΩ loads, and the power density of the two MPTs was 53.1 µW/cm^3.

Table 1 compares different microgenerator designs and technologies. Our system generally has better power density than other electromagnetic approaches. The MEMS capacitor and piezoelectric approaches have better power density. We modeled two coils as an AC source, with internal resistance R_{int} = 1,030Ω. Using this model, we performed several PSpice simulations with different voltage multipliers (a doubler, a tripler, and a quadrupler) to find the one that would

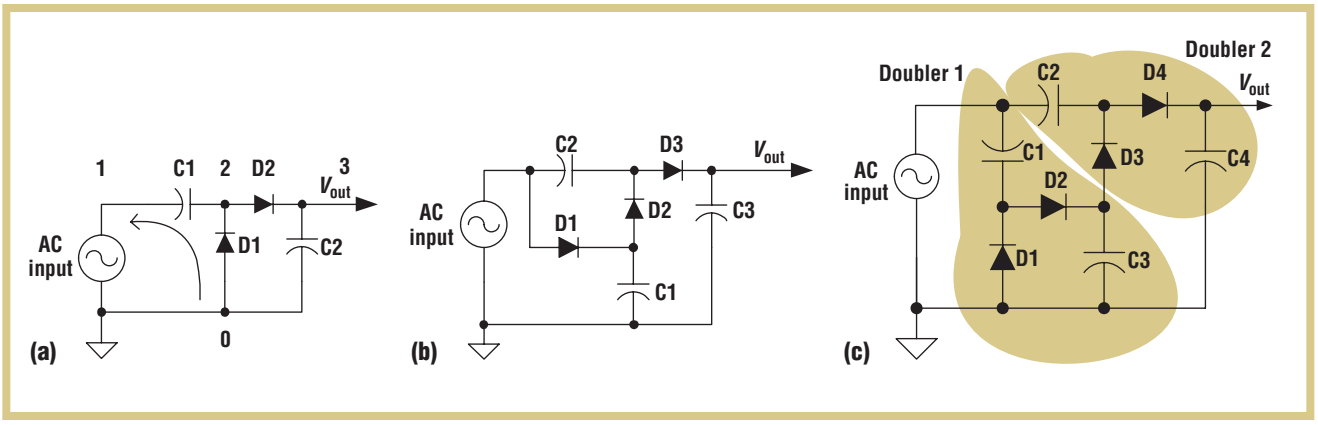

Figure 3. Schematics of a voltage (a) doubler, (b) tripler, and (c) quadrupler.

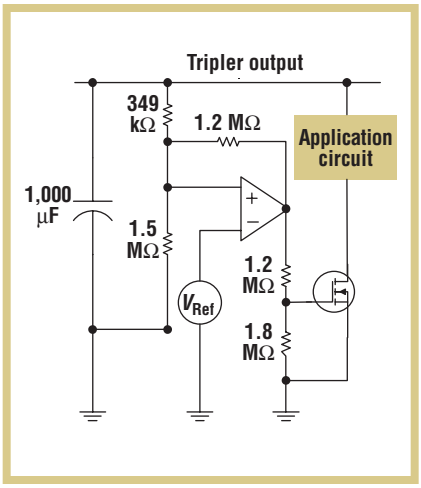

Figure 4. The startup circuit. (Reference voltage Vref sets the circuit's threshold voltage. The voltage multiplier here is a tripler.)

best meet our output voltage and power requirements.

The following performance metrics can help quantify the converters' performance:

- *Available stored energy*. The MPG doesn't usually generate enough power for continuous use. It stores input energy on a storage capacitor and releases it as necessary. This method is the *duty-cycled approach*. Leakage issues aside, you can apply the MPG to any off-the-shelf circuit with the startup circuit, provided that circuit's average power consumption is lower than the MPG's and the storage capacitor is large enough. The startup circuit controls the amount of energy stored in storage capacitor $C_{storage}$ through $V_{th}(H)$ and $V_{th}(L)$. Available stored energy is the stored energy available to the application circuit; we calculate ASE using equation 4.
- *Startup time*. ST is the elapsed time required to charge the storage capacitor's potential from 0 to $V_{th}(H)$ using the MPG.
- *Recharge time*. RT is the elapsed time required to charge the storage capacitor from $V_{th}(L)$ to $V_{th}(H)$ using the MPG.
- *Average input power*. Input energy (IE) is necessary to charge $C_{storage}$ from low threshold voltage $V_{th}(L)$ to high threshold voltage $V_{th}(H)$. Average input power is the input energy per unit charge time. Mathematically, $AIP = IE/RT$. Lower AIPs are desirable.
- *Energy efficiency*. EE is the available stored energy per unit of input energy. Quantitatively, $EE = (ASE/IE) \times 100\%$. Higher EE means better performance.
- *Output load (capacitive and resistive)*. The voltage multiplier's output connects to a storage capacitor and a resistive load. A duty-cycled approach requires a large storage capacitor, typically 1,000 µF, so the load is predominantly capacitive. The resistive load represents the load from the startup circuit and the application circuit in shutdown (sleep) mode. Typical loads are small, in the range of 50 to 500 kΩ (equivalent to the startup circuit's load). We didn't include the energy dissipated in the resistive load when calculating the output power.

We performed several PSpice simulations with a test voltage multiplier, source resistance R_{int}, and an AC source (V_{p-p} = 2.4 V, f = 70.6 Hz), choosing the parameters that best represent the actual MPG. The voltage multiplier's storage capacitor was 1,000 µF. We used three predefined groups of threshold voltages $V_{th}(L)$ and $V_{th}(H)$: (1.0 V, 1.4 V), (1.4 V, 1.8 V), and (1.8 V, 2.2 V), with ASE of 0.48 mJ,

TABLE 1
A comparison of different vibration-to-electrical transducers.

Design	Input amplitude or acceleration, and vibration frequency	Power output (power, output voltage V_{out})	Volume (cm^3)	Power density ($\mu W/cm^3$)	Technology
Williams et al.[6]	—	—	—	10–15	Electromagnetic
Amirtharajah and Chandrakasan[7]	2 cm, 2 Hz	400 µW, 180 mV rms (root-mean-square)	160	2.5	Electromagnetic
Meninger et al.[8]	2.52 kHz	8.6 µW	0.075	114.6	Microelectro-mechanical system capacitor
Roundy's first design[3]	2.25 m/s^2, 85 Hz	207 µW, 12 V DC	1	207	Piezoelectric
Roundy's third design[3]	2.25 m/s^2, 85 Hz	1,700 µW, 12 V DC	5.1	335	Piezoelectric
Two micro power transducers in series	4.63 m/s^2, 80 Hz	120 µW, 900 µV rms	2.262	53	Electromagnetic

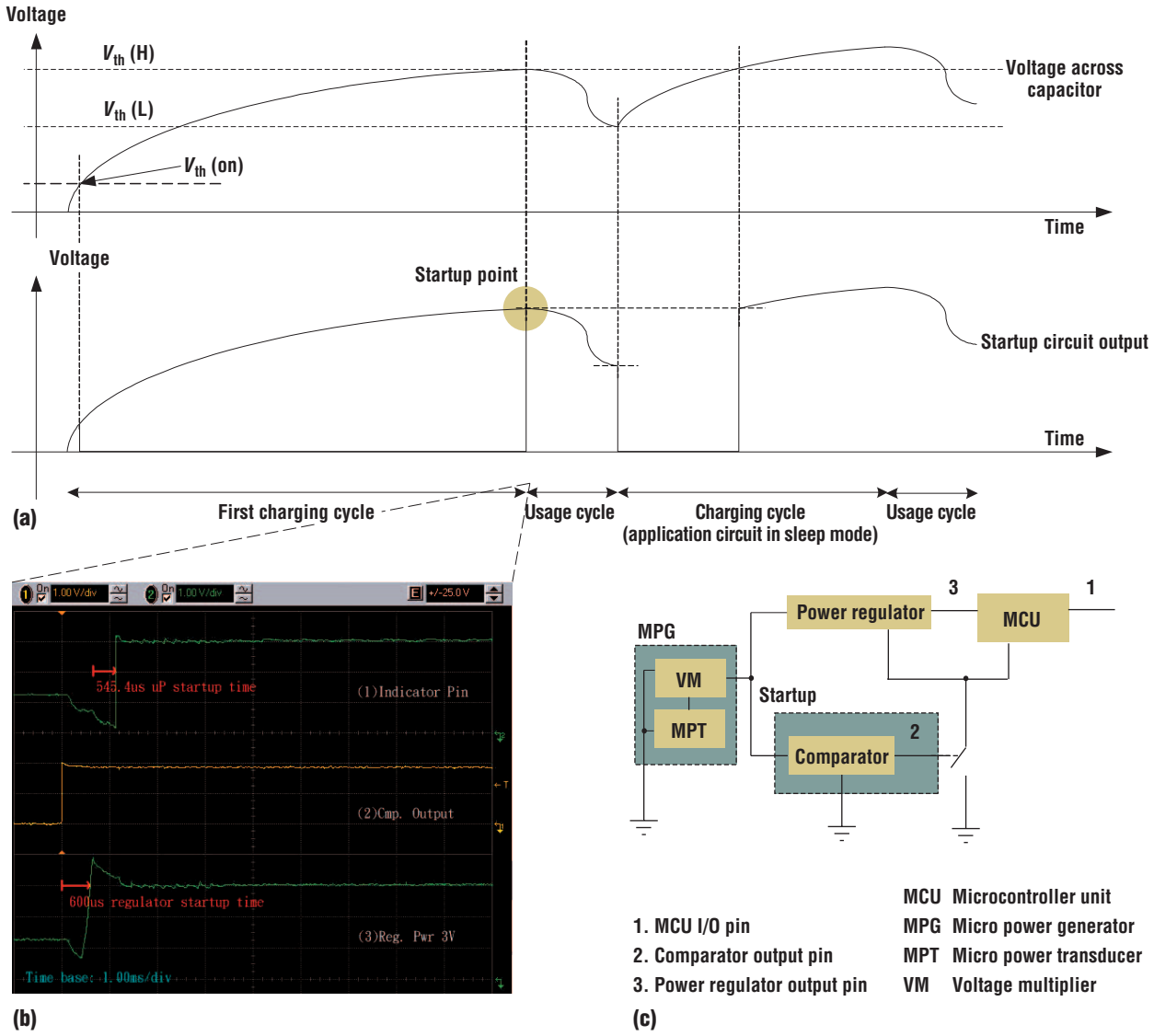

Figure 5. Transient response of the startup circuit and system supply during startup and usage: (a) input voltages to the startup circuit (top trace) and the corresponding startup circuit output (bottom trace), (b) an oscilloscope trace showing voltages at different points, and (c) a block diagram of the system.

0.64 mJ, and 0.8 mJ, respectively. Using PSpice, we compared voltage multipliers in terms of average input power, energy efficiency, startup time, and recharge time for different resistive loads. In general, low-order voltage multipliers have a lower input power than higher-order voltage multipliers. For example, for the same input energy stored on the storage capacitor, a doubler requires less input energy than a tripler or a quadrupler. However, the doubler can't achieve $V_{th}(H) \geq 1.8$ V under load. As Figure 6 shows, the tripler is more efficient than the quadrupler for converting power but takes slightly more time for startup and recharge.

We chose the tripler for the wireless thermometer application because it has the highest efficiency for ($V_{th}(H) = 1.8$ V, $V_{th}(L) = 1.4$ V). Its AIP is roughly 100 μJs^{-1}, which is approximately equal to the two MPGs' maximum power output. The tripler's startup time was approximately 32 seconds, with a recharge time of approximately 18 seconds for loads larger than 200 kΩ. Energy efficiency for average input power below 100 μW was 53 percent.

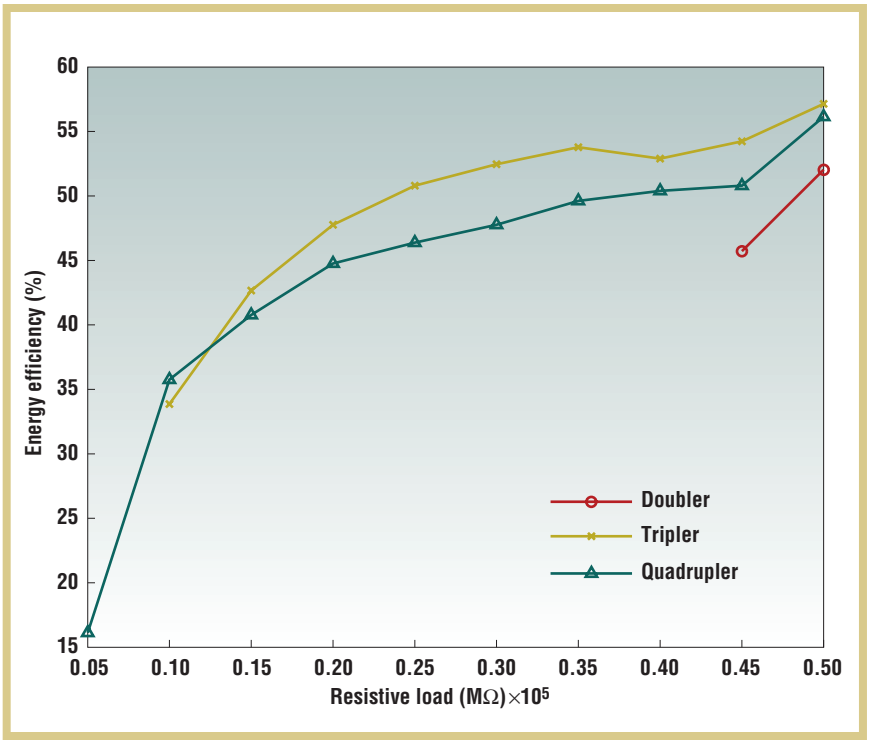

Figure 6. Energy efficiency versus resistive load for V_{th}(H) = 1.8 V and V_{th}(L) = 1.4 V (from PSpice simulations).

Wireless thermometer system

We developed an MPG-powered wireless thermometer to achieve the best power consumption, size, and component count. Figure 7 shows the system diagram for this thermometer. The system includes a Texas Instruments MSP430 microcontroller unit (MCU), a TI TMP100 temperature sensor, a custom-made surface acoustic wave (SAW) RF transmitter, and a TI TPS60311 charge-pump-based regulator. The MSP430 is a 16-bit MCU designed for ultralow-power applications. It has a long-period timer (3.67 s) clocked with a low-frequency crystal (76.8 kHz), and we connected its general-purpose I/O (GPIO) to the TMP100 for temperature readings. A custom-made SAW transmitter[9] gives a high degree of flexibility for controlling transmission power and antenna impedance matching. The transmitter operates at a carrier frequency of 433 MHz with a maximum transfer data rate of 4,800 bps. A compact helical antenna radiated the RF signal. The TMP100 thermometer chip (> 3 V), the MSP430 microcontroller (> 1.8 V), and the RF transmitter (> 3 V) require a 3 V power supply, so we used the charge pump regulator to further step up the 1.8 V input to 3.0 V. The regulator has an input range of 0.9 to 1.8 V and up to 90 percent efficiency, with a quiescent current consumption of 2 µA. It has a typical output ripple of 30 mV. We built the wireless thermometer with a startup circuit so that the MPG could connect directly to it.

The operating sequence is as follows:

1. When we vibrate the system, the MPG charges output storage capacitor C_{out}. We assume that the initial voltage of C_{out} is 0.
2. The startup circuit switches off the application circuit until the voltage across C_{out} rises higher than V_{th}(H), at which point the application circuit can operate.
3. The application circuit performs MCU initialization, temperature conversion, and data transmission.
4. After the application finishes, the circuit sleeps for a preprogrammed period and waits for the next activation if there's sufficient energy. Otherwise, it waits for the next charge-up of C_{out} above V_{th}(H).

We measured and analyzed the wireless thermometer's power consumption. We placed a 2.0 V power supply in series with a 22 kΩ resistor to emulate the MPG by limiting the current entering the 1,000 µF storage capacitor to 27 µA (at 1.4 to 2.0 V). We measured the instantaneous current consumption from the voltage across a 3Ω resistor, and we calculated the instantaneous power consumption by multiplying the current across the resistor by the voltage across the storage capacitor.

Table 2 shows the detailed measurements. The total energy consumed for a single activation was 212.62 µJ. Initial system startup and MCU initialization consumed 30 percent of the total energy. This consumption is avoidable for consecutive temperature measurements if the MPG generates more power than the application circuit consumes in sleep mode (22.38 µW). Temperature conversion consumed 17 percent of the total energy. Wireless transmission consumed the most energy: 53 percent; it took 1.42 s for a single measurement. While the MPG's storage capacitor charged, the system had a static power consumption of 4.5 µW. This is the minimum system current consumption, so the MPG must supply more than this amount to continuously operate the circuit.

The MPG directly powered the wireless thermometer. The startup circuit provided correct operation for 50 transmission cycles when we randomly applied vibration to the system. The startup circuit didn't apply power to the thermometer until the MPG raised the voltage on the 1,000 µF storage capacitor above 1.8 V. When the voltage exceeded this value, the startup circuit applied power to the wireless thermometer. The

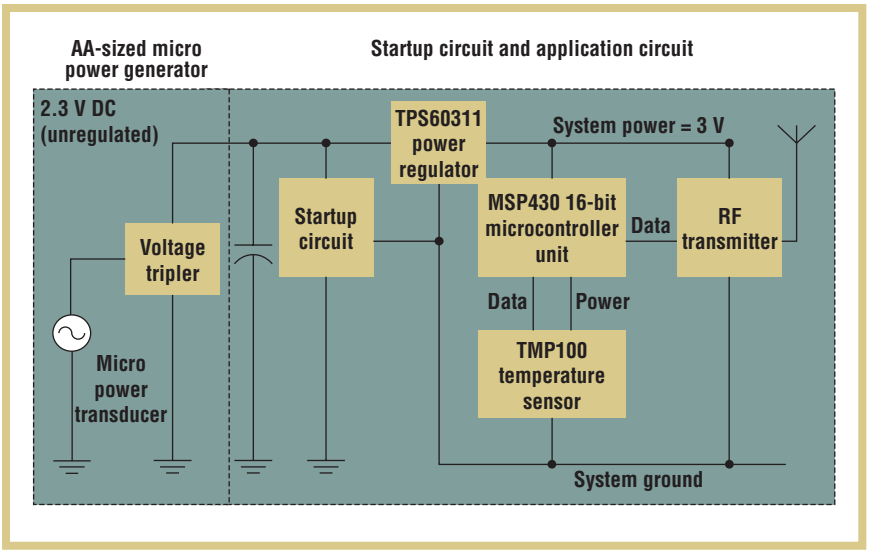

Figure 7. A system block diagram of a wireless-thermometer application.

MCU then acquired the temperature, transmitted it, and returned to sleep mode.

When the vibration on the MPG is continuous, the storage capacitor is large enough so that a single operation doesn't reduce the voltage across the storage capacitor to a value lower than 1.4 V. When the vibration stops, the voltage across the storage capacitor eventually falls below 1.4 V, at which time the startup circuit cuts power to the wireless thermometer circuit until it again reaches a value greater than 1.8 V.

The voltage regulator's startup time was 600 µs, and the MCU's startup time was 545.4 µs. For first-time activation, the MPG took 32 seconds to produce enough energy to drive the wireless RF thermometer with an input acceleration of 4.63 m/s^2 at 70.5 Hz. It took the MPG 18 seconds to generate enough energy for subsequent measurements. The RF transmission range between the host and the transmitter was 15 meters.

We are working to improve our generator's power output and reduce its size. As developments in microelectronics continue to reduce power consumption and motion-based generators improve in efficiency, we believe that this technology will become increasingly more pervasive. We expect to see vibration-powered devices in biomedical, sensing, data-logging, signal-processing, and consumer electronics applications in the future, because they have the compelling feature of not requiring batteries. P

ACKNOWLEDGMENTS

We thank the Hong Kong Innovation and Technology Commission, Brilliant System, DAKA Development, and Varitronix International for funding this project (ITF/185/01). We also greatly appreciate the Magtech Industrial Company (Hong Kong) for donating the permanent magnets needed for this project. Special thanks go to Thomas K.F. Lei and Gordon M.H. Chan for their contributions to this work.

REFERENCES

1. N.N.H. Ching et al., "A Laser-Micromachined Multi-modal Resonating Power Transducer for Wireless Sensing Systems," *Sensors and Actuators A: Physical*, Apr. 2002, pp. 685–690.
2. J.M.H. Lee et al., "Development of an AA Size Energy Transducer with Micro Resonators," *Proc. IEEE Int'l Symp. Circuits and Systems* (ISCAS 03), IEEE Press, 2003, vol. 4, pp. 876–879.
3. S.J. Roundy, *Energy Scavenging for Wireless Sensor Nodes with a Focus on Vibration to Electrical Conversion*, doctoral dissertation, Dept. of Mechanical Eng., Univ. of California, Berkeley, 2003; http://engnet.anu.edu.au/DEpeople/Shad.Roundy/paper/ShadThesis.pdf.
4. P. Horowitz and W. Hill, *The Art of Electronics*, 2nd ed., Cambridge Univ. Press, 1999.
5. "SOT23, 1.8V, Nanopower, Beyond-the-Rails Comparators with/without Reference," data sheet, Maxim Integrated Products, 1999; http://pdfserv.maxim-ic.com/en/ds/MAX917-MAX920.pdf.

TABLE 2
Energy consumption measurements for system startup and the application circuit.

Parameter	Time taken	Energy consumption (µJ)		Power consumption calculated
		Estimated	Measured	
Regular startup	600 µs	N/A	49.0	81.7 mW
Micro power startup	545 µs	N/A	15.0	27.6 mW
Temperature conversion	1.41 s	33.2	36.1	25.6 µW
Wireless transmission	4.17 ms	109	113	27.0 mW
Sleep (t = 30 s)	t	20t	22.4t	22.4 µW
Total energy consumption measured		(213.1 + 22.4t) = 884 µJ		
Average power consumption calculated		884/32 = 27.6 µW		

the AUTHORS

Steve C.L. Yuen is a principal engineer at Kontel Data System. He completed the work on the project described in this article while he was a graduate student at the Chinese University of Hong Kong. His research interests include mixed-signal IC systems and low-power sensor electronics. He received his MPhil in computer science and engineering from the Chinese University of Hong Kong. He's a member of the IEEE. Contact him at clyuen@kontel-data.com.

Johnny M.H. Lee is an engineer at SAE Magnetics. He completed the work on the project described in this article while he was a graduate student at the Chinese University of Hong Kong. His research interests include power microelectromechanical systems and optoelectrical design. He received his MPhil in mechanical and automation engineering from the Chinese University of Hong Kong. Contact him at johlee81@netvigator.com.

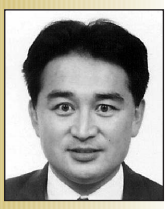

Wen J. Li is a professor in the Chinese University of Hong Kong's Department of Mechanical and Automation Engineering. His research interests include microelectromechanical systems and nanoscale sensors and actuators. He received his PhD in aerospace engineering from the University of California, Los Angeles. He's a member of the IEEE. Contact him at wen@mae.cuhk.edu.hk.

Philip H.W. Leong is a professor in the Chinese University of Hong Kong's Department of Computer Science and Engineering. His research interests include reconfigurable computing and signal processing. He received his PhD in electrical engineering from Sydney University. He's a senior member of the IEEE. Contact him at phwl@cse.cuhk.edu.hk.

6. C.B. Williams et al., "Development of an Electromagnetic Microgenerator," *IEE Proc. Circuits, Devices and Systems*, vol. 148, no. 6, 2001, pp. 337–342.

7. R. Amirtharajah and A.P. Chandrakasan, "Self-Powered Signal Processing Using Vibration-Based Power Generation," *IEEE J. Solid-State Circuits*, vol. 33, no. 5, 1998, pp. 687–695.

8. S. Meninger et al., "Vibration-to-Electric Energy Conversion," *IEEE Trans. Very Large Scale Integration Systems*, vol. 9, no. 1, 2001, pp. 64–76.

9. J. Nie, "SAW Based Transmitter Design Notes," 20 Aug. 2003; www.rfm.com/support/apnotes/sawbasedtransmitter.pdf.

For more information on this or any other computing topic, please visit our Digital Library at www.computer.org/publications/dlib.

Tried any new gadgets lately?

Any products your peers should know about? Write a review for *IEEE Pervasive Computing*, and tell us why you were impressed. Our New Products department features reviews of the latest components, devices, tools, and other ubiquitous computing gadgets on the market.

Send your reviews and recommendations to pvcproducts@computer.org